LETTERS

Near-Field Optical Imaging of Transient Absorption Dynamics in Organic Nanocrystals

Yuzhen Shen, Tzu-Chau Lin, Jianming Dai, Przemyslaw Markowicz, and Paras N. Prasad*

Photonics Research Laboratory, Institute for Lasers, Photonics and Biophotonics, Departments of Chemistry, Physics, Electrical Engineering, and Medicine, University at Buffalo, The State University of New York, Buffalo, New York 14260

Collection-mode near-field scanning optical microscopy is combined with femtosecond two-color pump−probe spectroscopy to study the transient absorption dynamics in organic crystals. The temporal evolution of the variation in the nonlinear transmittance of nanostructures is mapped with a spatial resolution of 200 nm and temporal resolution of 150 fs. Near-field time-resolved measurements indicate a nonradiative energy transfer from the excited molecules to the metal coating of a near-field probe.

Ultrafast measurements of dynamic processes in nanostructures require high resolution in both time and space. Time-resolved pump−probe techniques have been widely used in dynamic studies, in which a pump pulse excites a sample and modifies its absorption and refractive index, and a subsequent pulse probes the optical response of the sample. The dynamics of the excited-state population is measured from the probe transmittance or reflectance as a function of time delay between pump and probe pulses. The temporal resolution is limited by pump and probe pulse widths, and the development of ultrashort lasers has improved the temporal resolution to the femtosecond time scale. Conventional pump−probe measurements are performed in the far field. Due to the diffraction limit of pump and probe light, the information obtained is the average response over a macroscopic region. Recent advances in near-field scanning optical microscopy (NSOM)[1−5] overcome the diffraction limit and make it possible to combine this technique with ultrafast laser spectroscopy to probe optical interactions with femtosecond temporal resolution and nanometer spatial resolution. In fact, a few configurations combining femtosecond pump−probe technique with NSOM have been demonstrated, such as far-field pumping and near-field probing or both near-field pumping and probing, and used for carrier dynamics studies in semiconductors.[6−10] In these configurations, pump or probe

pulses are passed through a near-field fiber probe, where the dispersion compensation is necessary to compress the pulse width, and the alignment is delicate. In this Letter, we employ collection-mode NSOM[11,12] combined with femtosecond two-color pump−probe spectroscopy to study local transient absorption dynamics in organic nanostructures. In our study, both pump and probe pulses are sent to the sample in the far-field free space, and the transient transmittance of the probe pulse is detected in the near-field.

The schematic of the experimental setup is shown in Figure 1. A femtosecond self-mode-locked Ti:Sapphire laser, pumped with a frequency-doubled Nd:YVO$_4$ laser, is used as an excitation source at 800 nm with an average power of 1.5 W. The pulse width is 100 fs at a repetition rate of 80 MHz. The laser output is split into two beams. One beam at 800 nm is passed through a variable optical delay line as the pump, whereas the other beam is frequency doubled by a β-BaB$_2$O$_4$ (BBO) crystal to generate 400 nm light as the probe. Thus, two-photon absorption is used to create saturation of a level, and the saturation is probed by one-photon absorption to the same level. The pump power is controlled with a variable attenuator, and the probe power is set at 0.1 mW to minimize the probe-induced effect. The pump and probe beams are recombined at a dichroic beam splitter and then focused with an achromatic
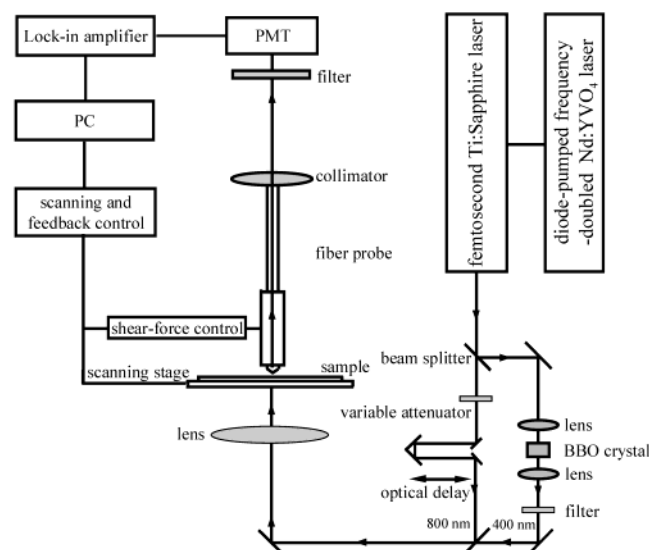
Figure 1. Schematic of the femtosecond time-resolved collection-mode near-field microscopy and spectroscopy.

lens onto the sample. The probe transmittance is collected by an aluminum-coated probe with an aperture of 50 nm in the near field above the sample, passed through an interference filter centered at 400 nm, and detected by a PMT connected to a computer to process data or generate an optical image. In a scan, the sample moves relative to the probe. Shear-force feedback using tuning fork detection keeps the probe–sample separation constant and also produces the topographic image simultaneously with the optical image as the sample stage is rastered beneath the fiber probe. The choice of using two-color instead of cross-polarized pump–probe techniques in the present time-resolved study is dictated by the fact that the optical fiber connected to the near-field probe and used for signal collection is not polarization-preserving and cannot achieve polarization discrimination between the pump and the probe. However, the wavelength difference between the pump and the probe allows us to prevent the pump light from reaching the detector and increases the signal-to-noise ratio.

The sample is prepared by spin coating a drop of dilute tetrahydrofuran (THF) solution of *N,N,N*-tris{4-{2-{4-[5-(4-*tert*-butylphenyl)-1,3,4-oxadiazol-2-yl]phenyl}-1-ethenyl}phenyl}-amine (abbreviated as PRL-701) on a BK-7 microscope cover slip. The solution is nanofiltered through a Teflon filter having a 0.2 μm pore size prior to the deposition. PRL-701 is a new two-photon chromophore synthesized in 32% yield by the reaction of the vinyloxadiazole compound with tribromotriphen-ylamine under palladium-catalyzed Heck conditions. It exhibits a large two-photon excitation cross section at ∼800 nm.[13] The PRL-701 crystallizes due to solvent evaporation. The crystals come out of solution so quickly that all of PRL-701 in the solution has precipitated before any of the nanocrystals can become large.

Figure 2a shows a 5 μm × 5 μm topographic image of two randomly distributed PRL-701 nanocrystals. The fwhm of the cross section is 200 nm in the nanostructures. The corresponding transient transmission images at two different time delays are presented in Figure 2b,c, respectively, which show that the intensity of transmission increases as the time delays approach zero. The intensity variations of transmitted field are correlated with the topographic features. The optical contrast arises from the variation in boundary conditions as the metal-coated probe scans from the near field of the uniform substrate surface to that of the nanostructures, in which the magnitude of the optical
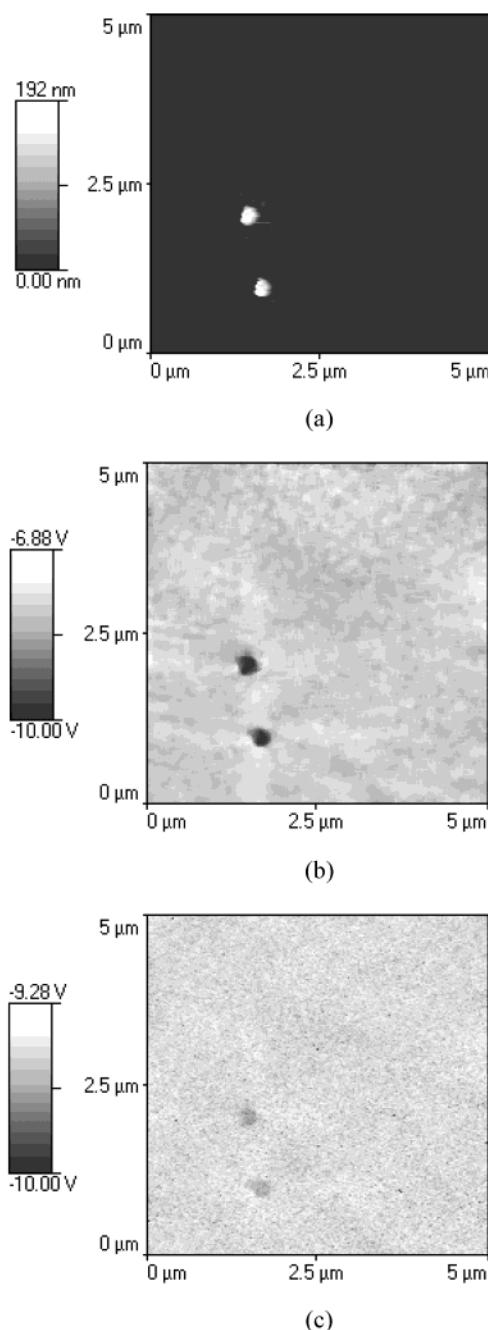
Figure 2. (a) Topographic image and (b) and (c) transient transmission images at time delay $\Delta t = 30$ and 0 ps, respectively.

field is more attenuated over these nanostructures than over the film. The reduced optical contrast from Figure 2b,c indicates that, in the presence of the high-peak-power pump pulse, the excited states are populated, and the depletion of the ground-state population leads to a decrease in the molecular transition from the ground state to the excited state. As a result, the absorption is saturated, the PRL-701 nanostructures become more transparent, and the optical contrast is reduced at sufficiently high excitation intensity. Therefore, saturation of absorption by two-photon excitation is established.

The transient transmittances of probe pulses for three different probe–sample distances, d, are shown in Figure 3. The transient transmittance is measured by locating near-field probe at a local site of the nanostructures and then detecting the transmitted probe intensities as a function of time delay between the pump and probe pulses. The 10−90% rise time demonstrates that the response time of transient absorption is ∼150 fs. The population
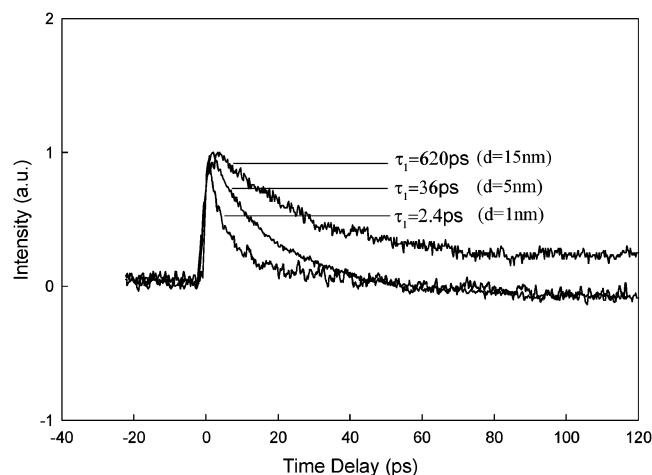
Letters

J. Phys. Chem. B, Vol. 107, No. 49, 2003 **13553**

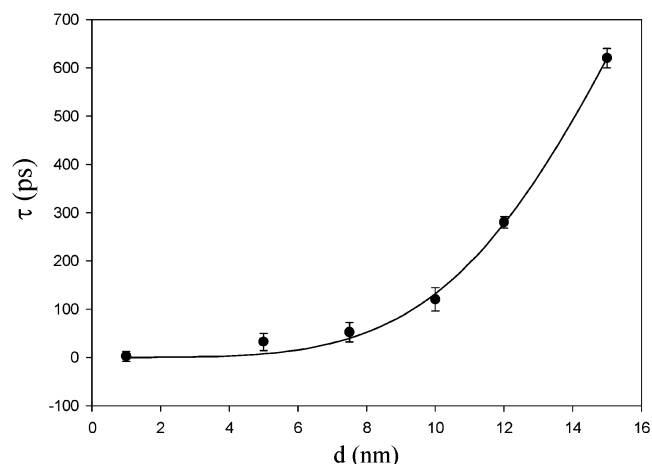**Figure 3.** Transient transmittace of PRL-701 nanostructure.

Figure 4. Distance dependence of excited-state relaxation time.

depletion is recovered in the time interval between two adjacent pump pulses. The distance dependence of the excited-state relaxation time, τ, is shown in Figure 4. The solid curve in Figure 4 is a best fit to the following function:

$$\tau = \tau_0 \frac{Ad^4}{B + Cd + Dd^4} \qquad (1)$$

which can be derived for dipole-metal surface interactions,[14,15] and where $A = 3.88 \times 10^{-15}/$ nm,[4] $B = 7.11 \times 10^{-10}$, $C = -2.35 \times 10^{-11}/$nm, and $D = 3.88 \times 10^{-15}/$nm;[4] $\tau_0 = 1.75$ ns is the excited-state decay time at an infinite distance from the metal surface. τ_0 was determined in a bulk PRL-701 sample using a Streak Camera in an independent measurement. Both Figures 3 and 4 indicate that the lifetime of excited-state population is reduced dramatically with decreasing probe–

sample distance. This reduction of excited-state lifetime is due to the interactions between the excited molecules and the metal coating of the near-field probe.[16] When excited molecules are located close to a metal layer, they can be treated as damped-harmonic dipoles, which decay either by spontaneous emission of photons or by nonradiative energy transfer to the metal layer. The probabilities for those two different processes depend on the distance between the excited molecules and the metal surface. Equation 1 indicates that the nonradiative decay rate is proportional to d^{-4} when excited dipoles are located in the near-field of the metal surface, and therefore, a smaller probe–sample distance significantly accelerates the relaxation rate. Equation 1 also implies that, with and increase of d to infinity, τ becomes independent of d and is equal to τ_0.

In summary, we have demonstrated the capability of combining ultrafast two-color time-resolved pump–probe spectroscopy with collection-mode near-field optical microscopy for optical imaging and spectroscopic studies of the transient absorption dynamics in organic nanostrucutres, with ∼200 nm spatial resolution and ∼150 fs temporal resolution. We have also demonstrated that the probe–sample distance can considerably perturb the relaxation of the excited-state population due to dipole interactions between the excited molecules and the metal coating of the near-field probe.

References and Notes

(1) Phol, D. W.; Denk, W.; Lanz, M. *Appl. Phys. Lett.* **1984**, *44*, 651.
(2) Liberman, K.; Harush, S.; Lewis, A.; Kopelman, R. *Science* **1990**, *247*, 59.
(3) Betzig, E.; Trautman, J. K.; Harris, T. D.; Weiner, J. S.; Kostalek, P. L. *Science* **1991**, *251*, 1468.
(4) Xie, X. S.; Dunn, R. C. *Science* **1994**, *265*, 361.
(5) McNeill, J. D.; Connor, D. B. O.; Barbara, P. F. *J. Chem. Phys.* **2000**, *112*, 7811.
(6) Levy, J.; Nikitin, V.; Kikawa, J. M.; Cohen, A.; Samarth, N.; Garcia, R.; Awschalom, D. D. *Phys. Rev. Lett.* **1996**, *76*, 1948.
(7) Smith, S.; Holme, N. C. R.; Orr, B.; Kopelman, R. *Ultramicrosc.* **1998**, *71*, 213.
(8) Nechay, B. A.; Siegner, U.; Genoud, F. M.; Schertel, A.; Keller, U. *Appl. Phys. Lett.* **1999**, *74*, 61.
(9) Guenther, T.; Emiliani, V.; Intonti, F.; Lienau, C.; Elsaesser, T. *Appl. Phys. Lett.* **1999**, *75*, 3500.
(10) Guest, J. R.; Stievater, Tt. H.; Chen, G.; Tabak, E. A.; Orr, B. G.; Steel, D. G.; Gammon, D.; Katzer, D. S. *Science* **2001**, *293*, 2224.
(11) Betzig, E.; Isaacson, M.; Lewis, A. *Appl. Phys. Lett.* **1989**, *51*, 2088.
(12) Shen, Y.; Swiatkiewicz, J.; Markowicz, P.; Prasad, P. N. *Appl. Phys. Lett.* **2001**, *79*, 2681.
(13) Chung, S. J.; Kim, K. S.; Lin, T. C.; He, G. S.; Swiatkiewicz, J.; Prasad, P. N. *J. Phys. Chem. B* **1999**, *103*, 10741.
(14) Drexahage, K. H. *Progress in Optics*; North-Holland; New York, 1974.
(15) Wokau, A.; Lautz, H. P.; Kiny, A. P.; Wild, U. P.; Ernst, R. R. *J. Chem. Phys.* **1983**, *79*, 509.
(16) Kopelman, R.; Shi, Z. Y.; Li, C. S. *J. Lumin.* **1991**, *48*, 143.